國立臺灣大學/國立嘉義高中科學班

個別科學研究成果報告

From Cusps to Cores: Quantifying the Impact of Stellar Feedback on Dark Matter Halos

學年度: 114 學年度

指導教授: 物理系 胡家瑜 老師

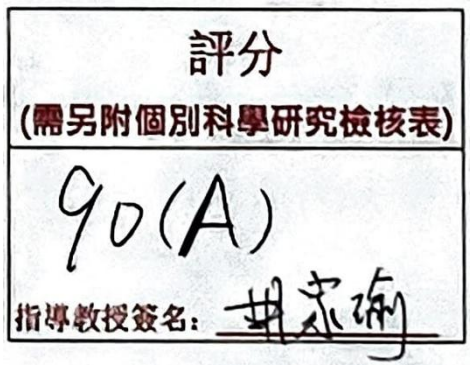

學生姓名: 何承祐

中 華 民 國 １１４ 年 4 月 ２７ 日

Table of Contents

List of Figures

摘要

星系暈尖點問題是天文物理中在小尺度下的難題。許多僅有暗物質的流體動力學模擬指出暗物質暈的密度分布在星系中央有尖點般的極大值，但觀測卻顯示該密度分布中央應是平坦的。我們使用高解析度的 GIZMO 程式碼，模擬單獨一個矮星系的演化，並探討有、無恆星反饋所造成的差異。為了定量分析平坦暗物質暈的形成，我們計算了密度分布$\rho \propto r^{-\gamma}$的指數γ、氣體分布的特徵高度，以及氣體流量及相應的載質量因子。我們發現恆星反饋對驅動氣體外流及形成平坦的暗物質核心至關重要。氣體外流雖然造成了暗物質斜率的變化，兩者在時序上並不直接耦合：前者和間歇性的恆星形成過程有關，後者變化卻較為平緩。此外，我們定量分析了核心形成的典型時間 $t_c \approx 0.65$ Gyr，以及載質量因子與密度分布的時序演化與強度。

Abstract

The cuspy halo problem is a long-standing small-scale challenge in astrophysics. While dark-matter-only hydrodynamical simulations show that the dark matter profile exhibits a central cusp, observations find a flat, core-like profile. We employ high-resolution GIZMO simulations of an isolated dwarf galaxy and investigate its evolution with and without stellar feedback. We measured the power law exponent γ of the inner dark matter halo slope $\rho \propto r^{-\gamma}$, the scale height of gas particles, the gas flow rates and the respective mass loading factors to quantify core formation. We conclude that stellar feedback is essential to gas outflow and the formation of the core profile. We find that while the flattening of the inner dark matter slope is driven by galactic outflows, the two processes exhibit distinct temporal characteristics; outflow rates are episodic, corresponding to the bursty nature of star formation, while the change in the dark matter slope is gradual. We provide quantitative analyses of the characteristic time of core formation $t_c \approx 0.65$ Gyr, time evolution and magnitude of mass loading factors and the density profile slope.

I. Introduction

The prevailing Lambda Cold Dark Matter (ΛCDM) cosmological model is the most widely accepted framework of the universe today (Bullock & Boylan-Kolchin, 2017). It consists of three main components: (1) the cosmological constant Λ, which is associated with dark energy; (2) cold dark matter (CDM), composed of massive ($m{\sim}100\ \mathrm{GeV/c^2}$, heavier than other types of dark matter described below) dark matter particles that have low energies such that they are non-relativistic; and (3) ordinary matter, also known as baryons (Deruelle & Uzan, 2018). All galaxies are embedded in dark matter halos, which provide the gravitational force necessary for the observed rotation curve of galaxies (Sofue & Rubin, 2000).

Besides CDM, there are other candidates for dark matter. Hot dark matter (HDM) is composed of light ($m{\sim}1\ \mathrm{eV/c^2}$) particles, and they remain relativistic (i.e. their velocity is close to the speed of light) until late in the evolution of the universe. However, HDM erases small-scale density fluctuations in the universe quickly, so if the universe is composed of it, the resulting structure would be inconsistent with what we observe today. Warm dark matter (WDM) has a mass ($m{\sim}1\ \mathrm{keV/c^2}$) between that of CDM and HDM. They have smaller velocities than HDM, making the formation of cosmic structure possible. Other options, such as weakly interacting massive particles (WIMPs), are also potential candidates. Nevertheless, the cold dark matter theory remains the most supported by current observations (Bozorgnia et al., 2024).

The ΛCDM model has successfully explained many fundamental problems, including the formation of the cosmic microwave background, the large-scale structure of the universe (via CDM), and the accelerated expansion of the universe (via Λ). Despite its success, the theory has faced challenges at scales smaller than roughly 1 megaparsec (1 Mpc) and halo masses below 10^{11} solar masses ($M_\odot$) (Bullock & Boylan-Kolchin, 2017).

One such issue is the cuspy halo problem, also known as the cusp-core problem. Many N-body numerical simulations show that the distribution of dark matter follows a Navarro–Frenk–White (NFW) density profile (Navarro et al., 1996) given by:

$$\rho(r) = \frac{\rho_0}{\left(\frac{r}{r_0}\right)\left(1+\frac{r}{r_0}\right)^2} \tag{1}$$

where $\rho(r)$ is the dark matter mass density at a radial distance of r from the center of the galaxy, while ρ_0 and r_0 are constants. Equation (1) describes a cusp-like profile, where the density rises sharply as r approaches 0, and diverges at $r = 0$. More specifically, $\rho \propto r^{-1}$ as $r \to 0$, in agreement with dark-matter-only (no baryonic feedback) simulations based on the ΛCDM model which find $\rho \propto r^{-\gamma}$ as $r \to 0$, where $\gamma \simeq 0.8{\sim}1.4$. This is, however, inconsistent with observations of nearby dwarf galaxies. Analysis of rotation curves typically yields shallower slopes of $\gamma \simeq 0{\sim}0.5$, which correspond to a nearly constant-density, core-like profile (Bullock & Boylan-Kolchin, 2017; Hunter et al., 2012). A

visual comparison between the cuspy NFW and cored Burkert profiles is shown in **Figure 1**. The Burkert profile (Liu et al., 2005) is often used to describe a cored dark matter halo:

$$\rho(r) = \frac{\rho_0}{\left(1 + \frac{r}{r_0}\right)\left(1 + \frac{r}{r_0}\right)^2} \tag{2}$$

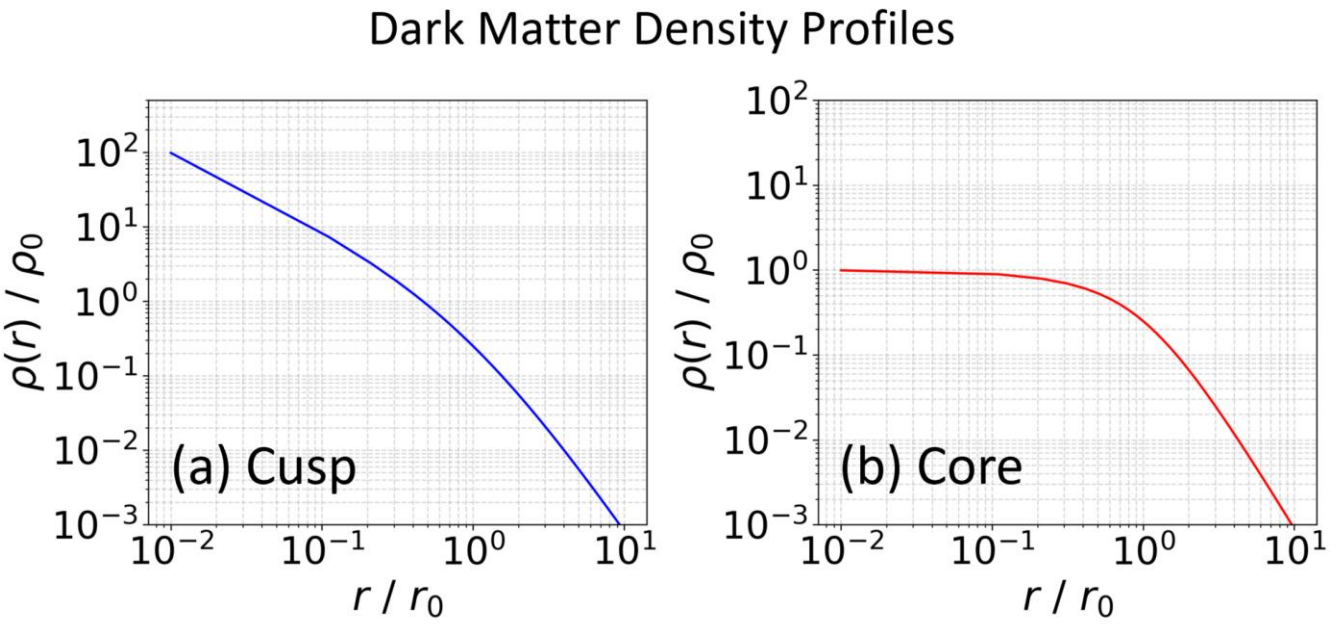

Figure 1: Comparison of dark matter halo density profiles.

(a) The cuspy NFW profile, described by Equation (1), exhibits a steep, divergent density toward the center, which occur in dark-matter-only hydrodynamic simulations. **(b)** The cored Bukert profile, described by Equation (2), shows a nearly constant central density, in better agreement with observational data from dwarf galaxies.

Various solutions have been proposed to resolve this issue. One category of solutions involve modifying the nature of dark matter, including warm dark matter and self-interacting dark matter (Del Popolo & Delliou, 2022). Another class of solutions focuses on baryonic physics. Stellar feedback is the process by which massive stars inject energy into the surrounding environment through events such as stellar winds and supernova explosions (Pontzen & Governato, 2012a). These events generate outflowing gas. Because dark matter interacts with baryonic matter through gravity, the outflowing gas can change the distribution of dark matter, flattening the cusp into a core. In other words, the fluctuating gravitational potential at the center transfers energy to the dark matter particles, enabling them to move outwards and forming a core-like profile.

Although previous studies have shown that stellar feedback does induce dark matter cores, the quantitative aspects of this process, such as the timescale of core formation, outflow rate of gas, and the inner slope of the dark matter profile as a function of time, remains an open area of investigation. In this work, we aim to address these gaps with high-resolution GIZMO simulations.

II. Research Objectives

A. To compare the simulated dark matter density profile with theory.
B. To quantify the evolution of the core-like dark matter profile over time.
C. To correlate the gas outflow with the variation of the slope of the inner dark matter profile.

III. Literature Review

Numerous dark-matter-only simulations of the formation of galaxies in the ΛCDM framework have revealed that the NFW profile is a universal description of dark matter halos (Bullock & Boylan-Kolchin, 2017; Navarro et al., 1996). However, these simulations neglected the effect of baryons. Without stellar feedback, the dark matter profile forms a cusp at the center.

Observations of the 21 cm emission line of neutral hydrogen (HI) enable astrophysicists to determine the rotation curves of galactic gas in a galaxy through the Doppler effect (de Blok & Bosma, 2002; de Naray et al., 2007; Hunter et al., 2012). By measuring the shift of the wavelength of this line, the rotational velocity can be mapped. The LITTLE THINGS project has used this to determine the dark matter profile of 41 galaxies (Hunter et al., 2012), and results show that real dark matter profiles have a constant-density core and rise more slowly near the center, as opposed to cusps found in dark-matter-only simulations (Bullock & Boylan-Kolchin, 2017). This inconsistency is referred to as the cuspy halo problem.

Baryonic feedback is a promising solution to this issue. Pontzen & Governato (Pontzen & Governato, 2012b) first showed that multiple, impulsive outflow events could turn cusps into cores. Hydrodynamical simulations showed that strong gas outflows can remove gas particles which have low angular momentum. Since these particles are more likely to sink towards the center of the galax y, this mechanism can erase the dark matter cusp (Governato et al., 2009). It has also been revealed that non-adiabatic, rapid outflows flatten cores by irreversibly transferring energy to dark matter particles. Additionally, in agreement with observations, only a small percentage of baryonic matter form stars, and star formation is bursty instead of continuous (Pontzen & Governato, 2012a). Recent simulations, including the FIRE simulations (Hopkins et al., 2017) and the NIHAO project (Wang et al., 2015),

aimed at modelling the stellar-to-halo mass ratio, which is the ratio of the total mass of stars to the total mass of dark matter in a galaxy.

Simulating galaxy formation is difficult since physical mechanisms occur across multiple scales, both spacially and temporally. To reduce computational cost, past studies have employed the sub-grid method: for unresolved scales, instead of simulating physical processes (e.g., supernova explosions) precisely, a sub-grid model is used to approximate its effect on larger scales. The sub-grid model has free parameters that can be tuned to match observations. However, it was found that using different stellar feedback models can lead to significantly different simulation results, thus making the sub-grid method less reliable (Scannapieco et al., 2012).

To reduce this uncertainty, the SMAUG project (C.-Y. Hu, 胡, Smith, et al., 2023) takes an alternative approach to avoid the sub-grid uncertainty. It uses high-resolution, small-scale simulations to directly resolve feedback from supernova explosions, a key physical process that regulates star formation and launch galactic outflows, and employs these models to simulate galaxy formation on a larger scale, improving the accuracy of the simulation. This work uses the GIZMO code (a part of the SMAUG project) to simulate a dwarf galaxy, which is computationally easier to simulate due to its small, faint nature.

IV. Methodology

A. Simulation Initial Conditions

The simulation resembles that of the Wolf-Lundmark-Melotte (WLM) galaxy, a well-studied, isolated dwarf galaxy (C.-Y. Hu, 胡, Sternberg, et al., 2023). Initial conditions were generated by the MAKEGALAXY code of Springel (Springel, 2005). The virial radius of the halo was $R_{vir} = 45$ kpc. Inside this region, the gravitational pull of the galaxy dominates that of the background density. More specifically, the average density inside R_{vir} is Δ times the background density, where $\Delta \sim 300$ is the overdensity threshold. Thus, the virial radius is a measure of the size of the galaxy. The virial mass, which is the total mass enclosed within the virial radius, is $M_{vir} = 10^{10}\ M_{\odot}$.

The halo initially followed a Hernquist profile (Hernquist et al., 1990):

$$\rho(r) = \frac{M}{2\pi}\frac{a}{r(r+a)^3} \tag{3}$$

where M is the total mass and a is a scale factor. The Hernquist profile was used because its total mass converges, while that of the NFW profile diverges. This property makes the Hernquist profile more suitable for numerical simulations.

The Hernquist proflie agrees with the NFW proflie near the center, but drops off more quickly at larger radius, since Equation (1) shows $\rho \propto r^{-3}$ when $r \to \infty$, while Equation (3) falls off as $\rho \propto r^{-4}$. **Figure 2** is a comparison of Equation (1) and Equation (3). The difference between the two profiles is also seen in $t = 0$ subplots in **Figure 5**.

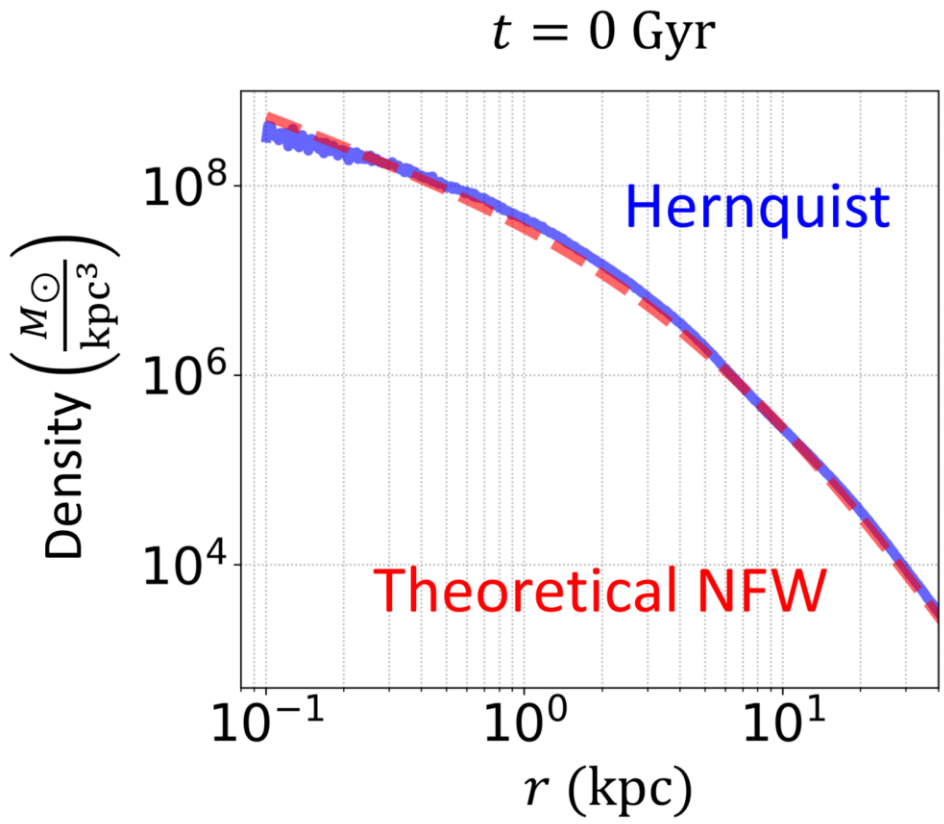

Figure 2: Comparison of the NFW and Hernquist density profiles.

Both profiles exhibit a central cusp with $\rho(r) \propto r^{-1}$ at small radii. The NFW profile is plotted with equation (1(1), while the Hernquist profile is obtained from the simulation initial conditions. Although the profiles are similar in the central regions, they diverge at large radii.

The baryonic mass fraction is 0.8%, indicating that only a small fraction of the total mass consists of normal matter. The total mass of stars is $10^7\ M_\odot$, while the total mass of gas is $7 \times 10^7\ M_\odot$, Both masses decay exponentially away from the center, with a scale length of 1 kpc. At the center, the surface density of gas is roughly $10\ M_\odot/\text{pc}^2$. The edge-on views of the galaxy, as shown in **Figure 3**, illustrates the visual structure of the galaxy

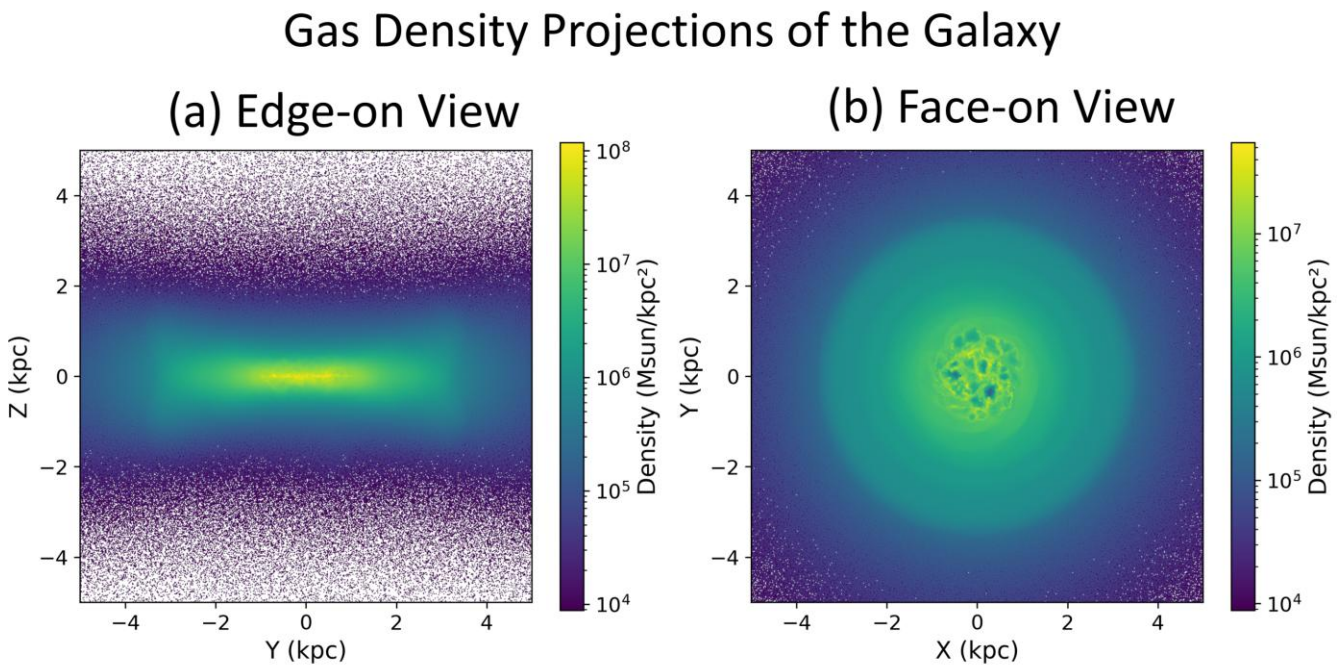

Figure 3: Edge-on and face-on views of the simulated galaxy.

The diagrams are generated by splitting the 5 kpc × 5 kpc area into 512 × 512 grids, and calculating the gas surface density in each grid. Color indicates the surface density. **(a)** YZ projection: the edge-on view shows a disk-like structure. Density decreases rapidly with Y and even more rapidly with Z. The vertical extent of the disk is approximately 4 kpc. **(b)** XY projection: the face-on view shows the radial structure of the galaxy. The central concentration and gradual drop in surface density reflect the exponential disk profile. The diagrams are plotted with data at $t = 0.02$ Gyr in Simulation I.

Simulation results are available as snapshots, which contain physical quantities of the system at a specific time. The time interval between snapshots is $10\,\mathrm{Myr}$, and the simulation terminates at ~ 800 Myr. In each simulation snapshot, the position (x, y, z) and velocity $(\dot{x}, \dot{y}, \dot{z})$ of each gas particle is available, with the center of the galaxy as the origin, and $z = 0$ as the galactic plane.

We ran two simulations. Simulation I included stellar feedback, such as supernova explosions. Simulation II, however, did not include stellar feedback.

B. Quantifying Core Formation

We quantified the gas outflow with the scale height mass flow rates. If we assume that the mass of gas per unit height $\rho(z) \propto e^{-z/h}$ is an exponentially decreasing function of z with scale height h, the total mass enclosed within the two planes $z = \pm h$ is:

$$M_{enc,h} = 2\int_0^h \rho(z)dz = \left(1 - \frac{1}{e}\right) M_{tot} \tag{4}$$

where M_{tot} is the total mass of gas particles. We use Equation (4) to determine the scale height h in each simulation snapshot. If there is gas outflow, the scale height should increase over time.

Mass flow rates and mass loading factors are useful quantities for analyzing core formation (C. Y. Hu, 2019). The net mass flow rate $\dot{M}$ is used to quantify the flow of gas:

$$\dot{M} = \dot{M}_{out} - \dot{M}_{in} \tag{5}$$

where $\dot{M}_{out}$ is the mass outflow rate, and $\dot{M}_{in}$ is the mass inflow rate. To calculate $\dot{M}_{out}$ and $\dot{M}_{in}$, we selected all the gas particles whose distance to the galactic plane $z = 0$ is between $z_0 - \frac{\mathrm{d}z}{2}$ and $z_0 + \frac{\mathrm{d}z}{2}$, where $z_0 = 2.0$ kpc is a chosen reference distance and $\mathrm{d}z = 0.1z_0$. For the particles within the slab $z \in [z_0 - \frac{\mathrm{d}z}{2}, z_0 + \frac{\mathrm{d}z}{2}]$, those with velocity z-component $\dot{z} > 0$ are counted in $\dot{M}_{out}$, while those with $\dot{z} < 0$ are counted towards $\dot{M}_{in}$. Conversely, for the particles within $z \in [-z_0 - \frac{\mathrm{d}z}{2}, -z_0 + \frac{\mathrm{d}z}{2}]$, those with $\dot{z} < 0$ are counted towards $\dot{M}_{in}$ and those with $\dot{z} > 0$ are counted in $\dot{M}_{out}$. $\dot{M}_{out}$ is computed as:

$$\dot{M}_{out} = \sum_i \frac{m_i v_{z,i}}{\mathrm{d}z} \tag{6}$$

where the summation is taken over the particles near $z = z_0$ with a positive z velocity, and those near $z = -z_0$ with a negative z velocity. Similarly, $\dot{M}_{in}$ is calculated as:

$$\dot{M}_{in} = -\sum_i \frac{m_i v_{z,i}}{\mathrm{d}z} \tag{7}$$

where the summation is taken over the particles near $z = z_0$ with a negative z velocity, and those near $z = -z_0$ with a positive z velocity. The negative sign in Equation (7) ensures that $\dot{M}_{in}$ is positive. We divide by $\mathrm{d}z$ so that the flow rates don't scale up when the height of the chosen slab increases. At the same instant, a different choice of z_0 may yield different flow rates. We did not impose a constraint on the distance of gas particles from the galactic center, as the majority of them are naturally concentrated within 5 kpc, as observed in **Figure 3**.

We normalize the flow rates by the star formation rate (SFR) of the galaxy to obtain a dimensionless quantity, the mass loading factor η. The outflow mass loading factor and inflow mass loading factor are computed as:

$$\eta_{out} = \dot{M}_{out}/\mathrm{SFR} \tag{8}$$

$$\eta_{in} = \dot{M}_{in}/\mathrm{SFR}. \tag{9}$$

The age of each star is available in the simulation snapshots. At each snapshot, it was calculated by summing the mass of stars younger than 10 Myr, providing a measure for star formation activity as a function of time. However, to reduce the impact of short-term fluctuations, we used the SFR averaged over the entire simulation time span, as shown in **Figure 8**.

The inner slope of the dark matter profile follows the power law $\rho \propto r^{-\gamma}$. We performed a linear regression between ρ and r to determine the value and uncertainty of γ. This methodology is explained in greater detail in **Figure 4**.

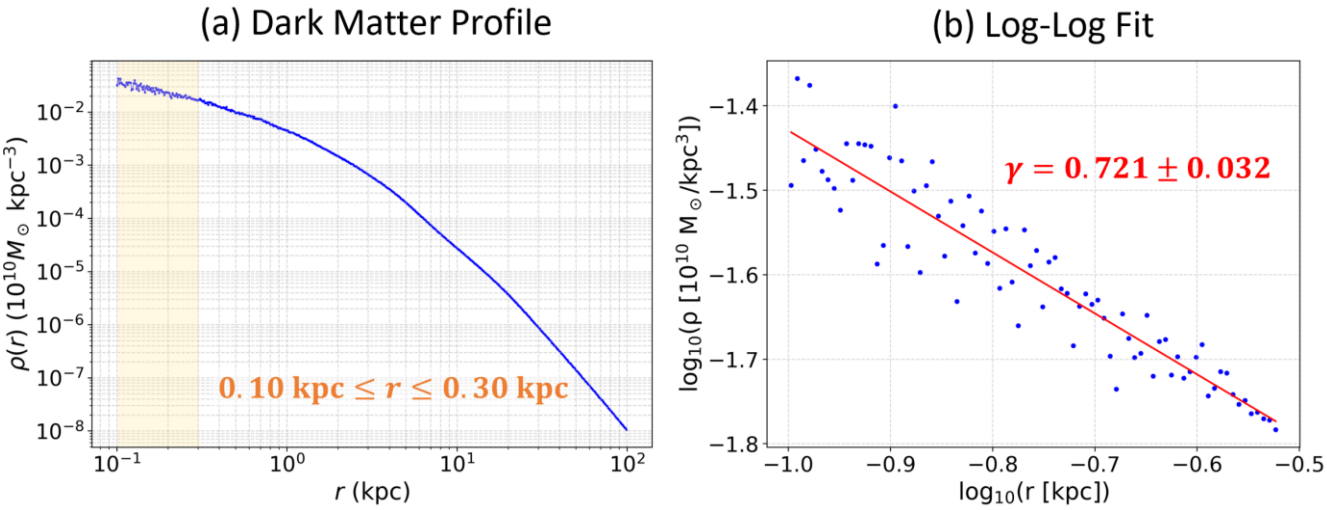

Figure 4: Methodology of finding the power law exponent γ.

This figure was generated at $t = 0$ Gyr in Simulation I. **(a)** Dark matter density as a function of radius. **(b)** Log-log plot of density and radius of the inner region $0.10\ \mathrm{kpc} \leq r \leq 0.30\ \mathrm{kpc}$. The slope of the best linear fit of this plot is $-\gamma$. We used scipy.stats.lingress in Python to calculate the regression.

V. Results and Discussion

A. Formation of Core Profile Over Time

Figure 5 shows the time evolution of the dark matter density profile under two different simulations. In both cases, the initial profile at $t = 0$ roughly agrees with the NFW form of Equation (1). However, depending on whether stellar feedback is considered, the evolution of the dark matter profile differs significantly. The simulation of panel **(a)** includes stellar feedback. Over time, the central region gradually flattened. At $t = 800$ Myr, the inner 0.5 kpc was nearly a constant-density region. In contrast, the simulation of panel **(b)** did not consider stellar feedback, and the simulated dark matter profile did not change significantly over the simulation time range.

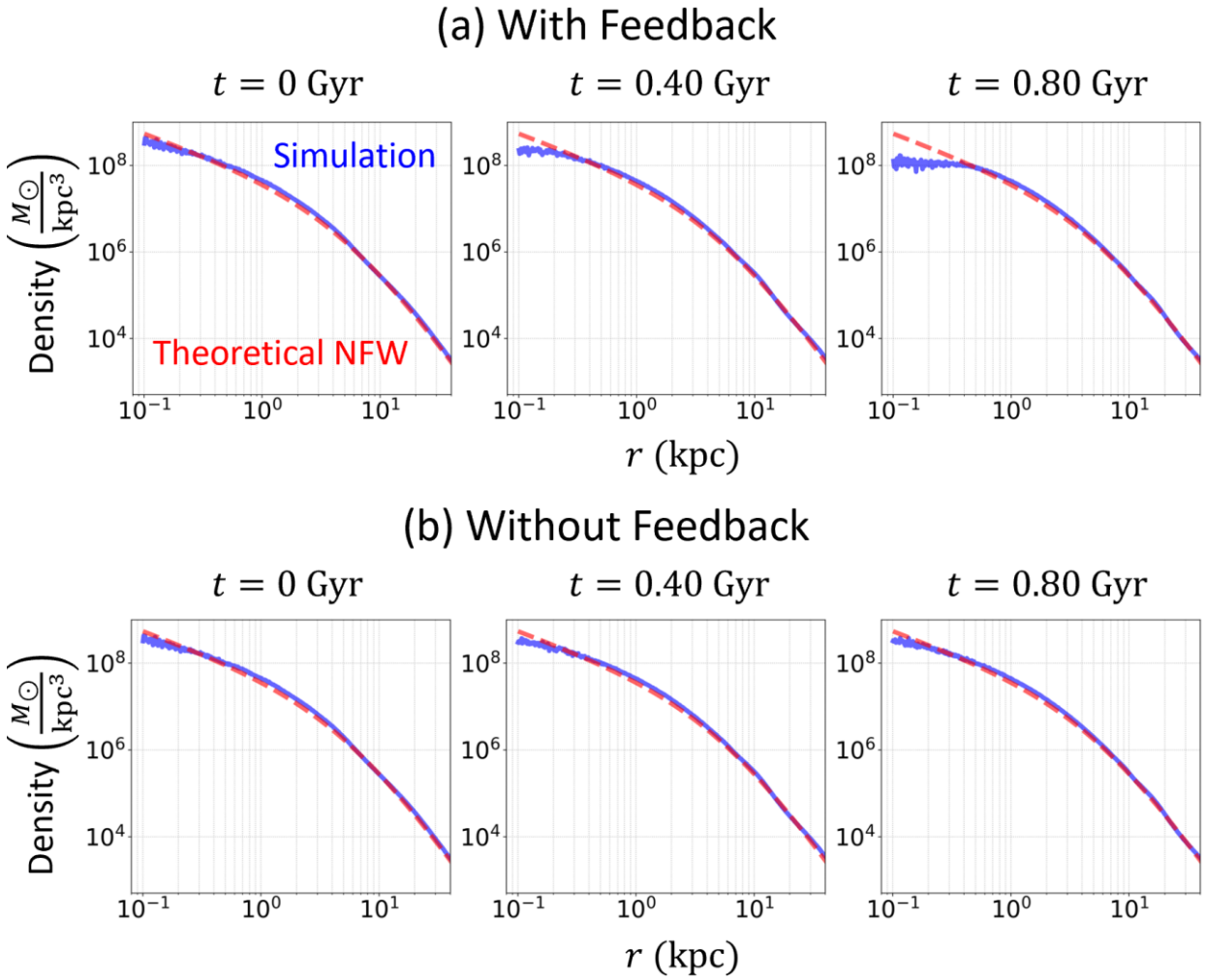

Figure 5: Evolution of dark matter density profiles in simulations with and without stellar feedback.

(a) With stellar feedback, the profile initially followed the cuspy Hernquist profile (approximately the NFW form of Equation (1)) at $t = 0$, but gradually flattened into a core. **(b)** Without stellar feedback, the profile remained cuspy throughout the simulation.

The evolution of the power law exponent γ in $\rho \propto r^{-\gamma}$ is plotted in **Figure 10**. We observe that γ in Simulation I decreased with time until reaching $\gamma \approx 0$ by the characteristic time $t_c \approx 0.65$ Gyr, while γ in Simulation II did not change significantly over the simulation time span, suggesting that the dark matter profile remained cuspy.

As shown in **Figure 6**, the edge-on views provide a clear picture of the episodic gas outflow caused by stellar feedback. This is quantified with the scale height and the mass loading factor described in the next section.

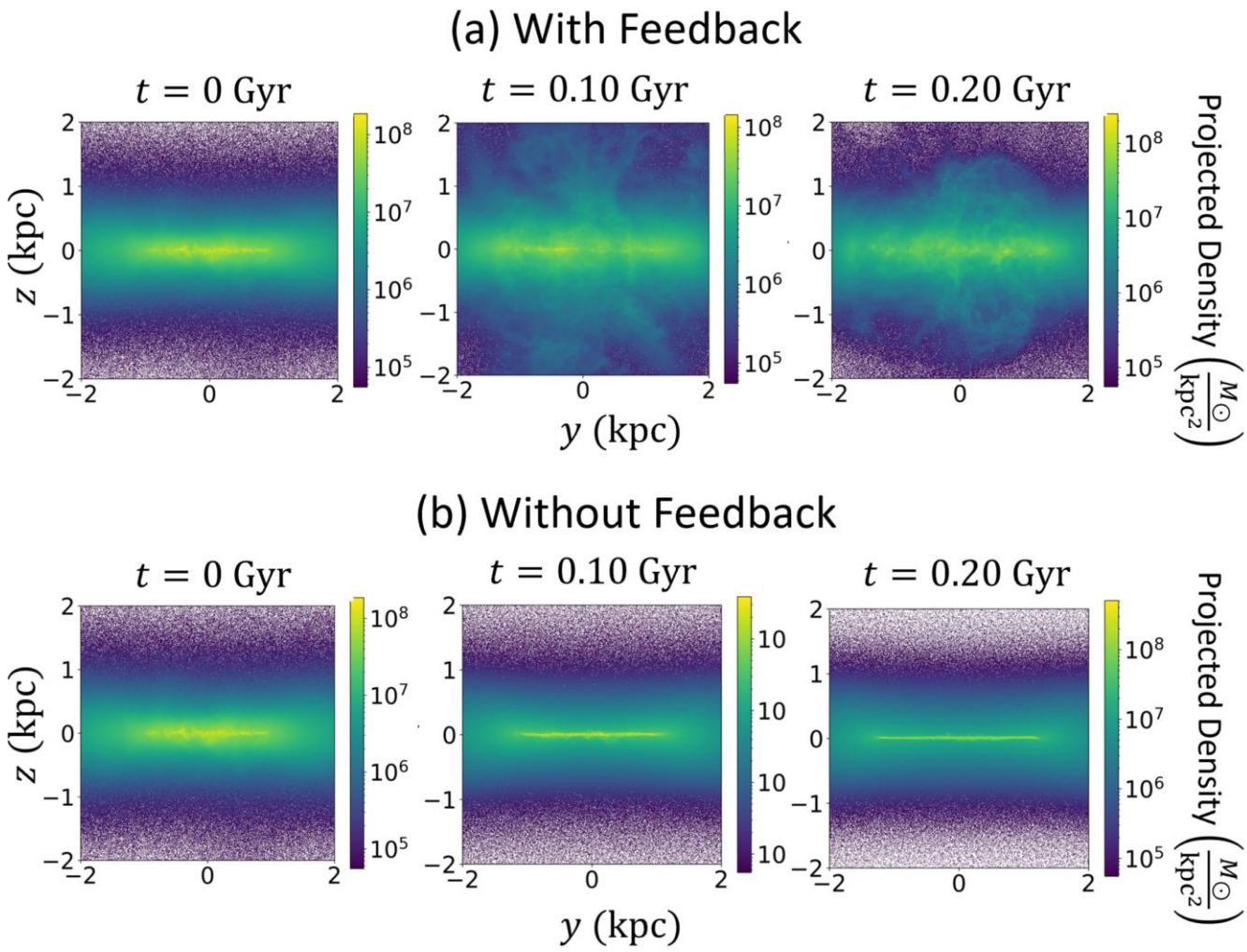

Figure 6: Edge-on views of the galaxy at $t = 0, 0.10, 0.20$ Gyr for both simulations.

(a) Simulation I evidently exhibits episodic gas outflow, with gas being visibly expelled from the center at $t = 0.10, 0.20$ Gyr. **(b)** Simulation II did not include stellar feedback, and no gas outflow is observed from the edge-on view.

This result highlights the well-established understanding that baryonic feedback plays a critical role in shaping dark matter halos. However, to gain deeper insight into the underlying mechanism, it is essential to investigate the dynamics of gas outflows.

B. Gas Outflow and the Inner Slope of the Dark Matter Profile

The disk's scale height h is determined such that the total mass enclosed by the two planes $z = \pm h$ is $1 - \frac{1}{e} \approx 63\%$ of the total mass of gas particles. This is a simple quantitative measure of gas outflow. **Figure 7** presents the time evolution of the scale height for both simulations. We observe that stellar feedback drives gas outflow in intermittent bursts. The scale height in the simulation with stellar feedback increases more rapidly than in the simulation without it, highlighting how stellar feedback enhances gas expulsion from the disk.

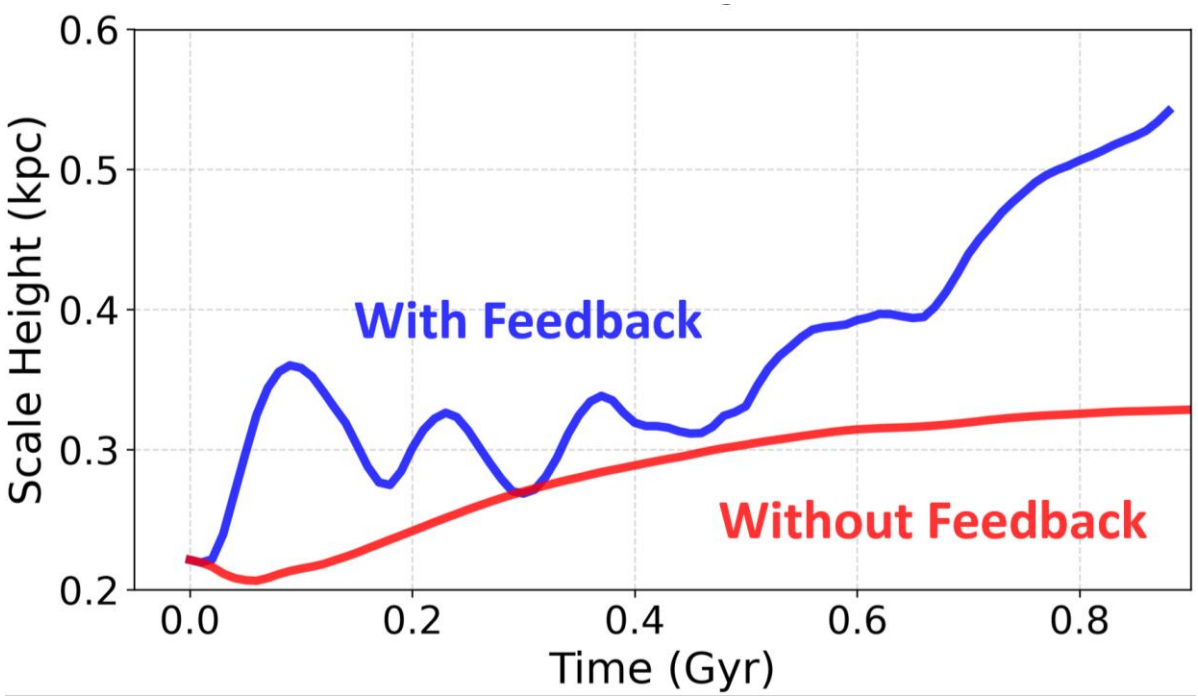

Figure 7: Evolution of gas scale height over time for both simulations.

In the simulation with stellar feedback, the scale height exhibits intermittent increases and grows more rapidly compared to the simulation without feedback. The scale height begins to differ dramatically after $t = 0.50$ Gyr. This highlights the role of stellar feedback in driving gas outflow.

We use the star formation rate (SFR) to calculate the dimensionless mass loading factor. **Figure 8** compares the evolution of the SFR in two simulations: one with stellar feedback (Simulation I) and one without (Simulation II). In Simulation I, there is episodic star formation. In other words, the rate which stars are formed has occasional bursts. In contrast, Simulation II lacked feedback mechanisms, allowing gas to cool and collapse continuously. As a result, star formation increases early on and then slowly declines. The average SFR of simulation I is $2.81 \times 10^{-4} \frac{10^{10}\ \mathrm{M}_\odot}{\mathrm{Gyr}}$, while the average SFR of simulation II is $3.40 \times 10^{-4} \frac{10^{10}\ \mathrm{M}_\odot}{\mathrm{Gyr}}$. We used these two values to calculate the mass loading factor.

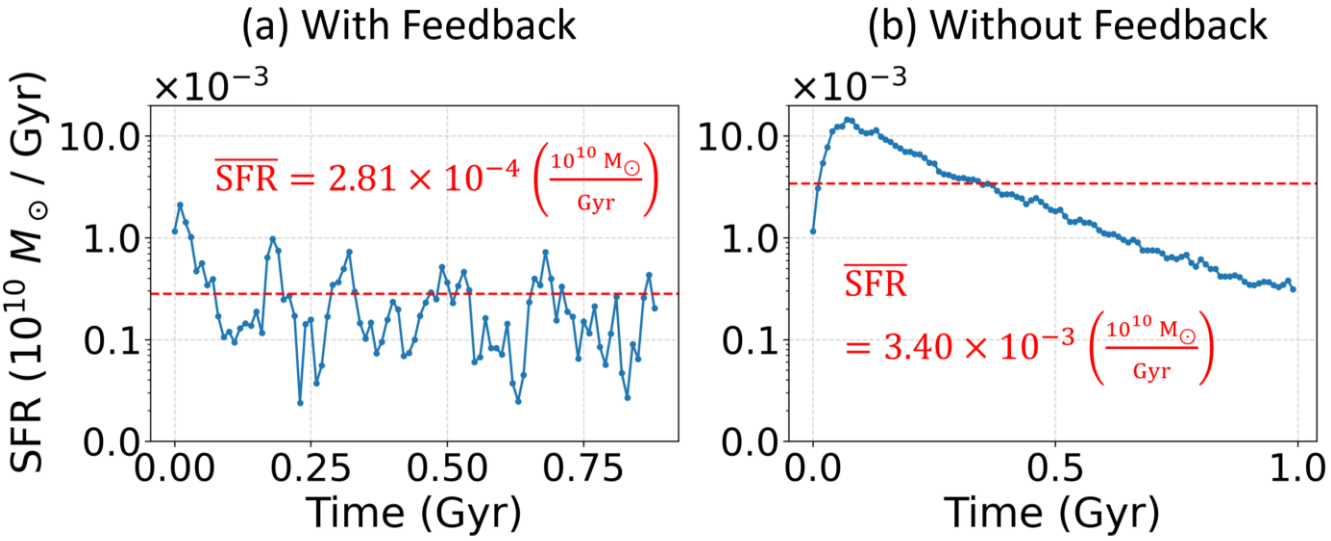

Figure 8: Star formation rate (SFR) over time with and without stellar feedback.

(a) With stellar feedback, the SFR of Simulation I has episodic bursts and averages at $2.81 \times 10^{-4} \frac{10^{10}\ \mathrm{M}_\odot}{\mathrm{Gyr}}$. **(b)** The SFR of Simulation II rises to a maximum near 0.1 Gyr and gradually decreases due to the lack of stellar feedback. It averages to $3.40 \times 10^{-4} \frac{10^{10}\ \mathrm{M}_\odot}{\mathrm{Gyr}}$.

The time evolution of the mass loading factors η_{out}, η_{in}, and $\eta_{\mathrm{net}} = \eta_{\mathrm{out}} - \eta_{\mathrm{in}}$ are shown in **Figure 9**. The episodic gas flow in Simulation I was quantified with the time-changing net mass loading factor η_{net} in Simulation I. On average, the magnitude of gas outflow is greater than that of gas inflow, generating a net outflow of gas, which redistributes the dark matter and turns the cusp into a constant-density core, as quantified in **Figure 10**. An outflow occurs roughly every $\Delta t \sim 0.1\mathrm{Gyr} - 0.2$ Gyr. The mass loading factor is of order $\eta \sim 10$, indicating strong outflow. In contrast, there is no episodic flow in Simulation II, and the overall effect is that gas flows in with $\eta \sim 0.01$. As a result, the cuspy dark matter profile remains.

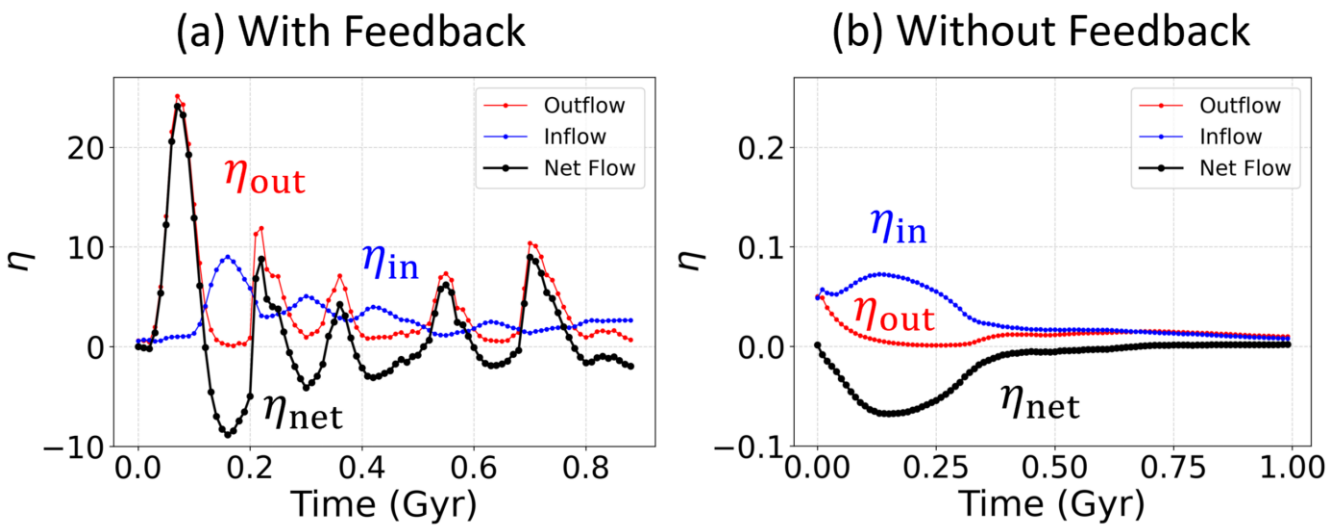

Figure 9: Evolution of outflow mass loading factor $\eta_{\rm out}$, outflow mass loading factor $\eta_{\rm in}$, and net mass loading factor $\eta_{\rm net} = \eta_{\rm out} - \eta_{\rm in}$ for both simulations.

The vertical scale between the two subplots differ by a factor of 100, highlighting the drastic difference between the outflow rates with and without feedback. **(a)** Simulation I: Strong, intermittent bursts of gas flow are observed from the time-varying mass loading factors. **(b)** Simulation II: There was initially small gas inflow, which decreases with time and approached zero. No episodic flow is observed.

Figure 10 compares the dark matter profile power law exponent γ with the net mass loading factor $\eta_{\rm net}$. In Simulation I, the exponent gradually decreased, while gas flow is episodic. Note that even though gas flows in irregular bursts, the change in the slope of the dark matter profile is gradual. In other words, the decrease of γ and the outflow of gas are decoupled. Interestingly, there is no obvious correlation between γ and $\eta_{\rm net}$ in the figure in both simulations, as there is no significant decrease in γ immediately following a strong outflow. However, by comparing the two simulations, it is evident that episodic gas outflow is crucial to the formation of the core profile.

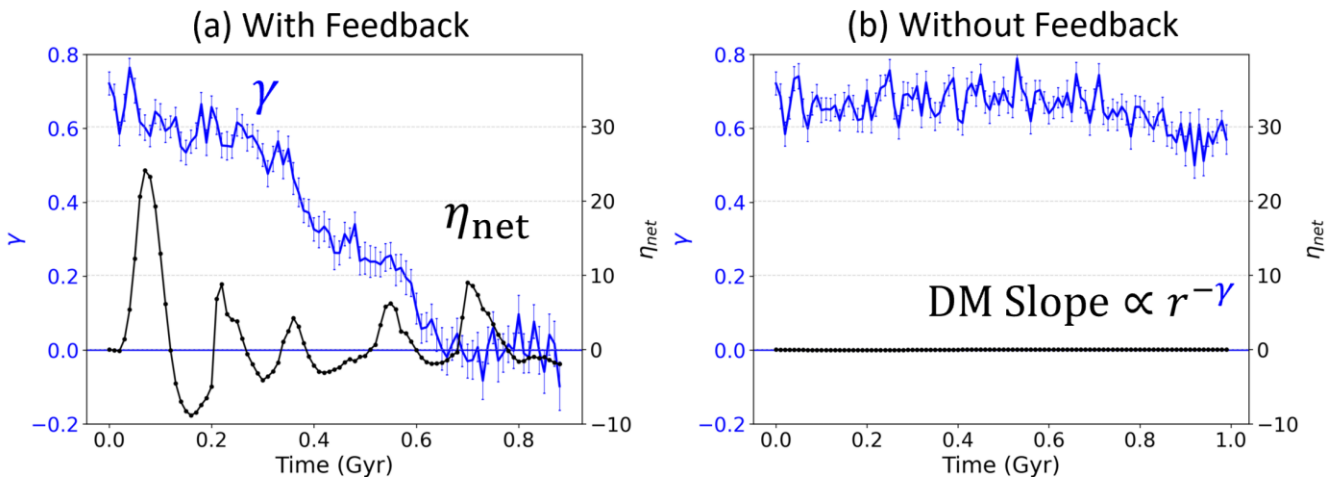

Figure 10: Evolution of dark matter profile exponent γ and net mass loading factor $\eta_{\rm net}$ for both simulations.

(a) Simulation I: γ gradually decreases, and $\eta_{\rm net}$ shows episodic behavior, with strong gas outflow as the overall effect. **(b)** Simulation II: γ roughly remains constant, while $\eta_{\rm net}$ initially exhibits a small net inflow and approaches zero over time.

VI. Conclusion

In this study, we used high-resolution GIZMO hydrodynamic simulations of a WLM-like dwarf galaxy to investigate the role of stellar feedback in shaping dark matter halos and provide a quantitative analysis of the cuspy halo problem. We ran two simulations: Simulation I, which included stellar feedback, and Simulation II, which did not include stellar feedback. Our main findings are summarized as follows.

A. Core Formation Requires Stellar Feedback

The initial condition of both simulations were identical. Both simulations had their dark matter density profiles initially cuspy and approximately following the theoretical NFW profile, with the power law exponent $\gamma \approx 0.7$ in $\rho \propto r^{-\gamma}$. With stellar feedback, the dark matter profile of Simulation I flattened into a core over time (**Figure 5**), and γ gradually decreased to nearly 0 at the characteristic time of core formation $t_c \approx 0.65$ Gyr (**Figure 10**). However, without stellar feedback, the density profile of Simulation II remained cuspy, and γ did not vary significantly from its initial value through the 0.80 Gyr run. Thus, we conclude that stellar feedback is essential to core formation.

B. Stellar Feedback Drives Gas Outflow

We used the scale height h and mass loading factors η to quantify gas outflow. Two planes at $z = \pm h$ enclsoe a constant fraction of the total mass of gas particles. Thus, the scale height is positively correlated with the outflow of gas. The mass loading factors are calculated by dividing the respective mass flow rates by the star formation rate, providing a dimensionless quantity to analyze gas outflow.

The density projections of both simulations (**Figure 6**) evidently reveal that gas outflow is significant in the simulation with stellar feedback. The evolution of the scale height (**Figure 7**) in Simulation I also exhibits intermittent increases and grows faster compared to Simulation II. Moreover, the evolution of the mass loading factor (**Figure 9**) in the simulation with stellar feedback demonstrates strong ($\eta \sim 10$), episodic gas outflow with period $\Delta t \sim 0.1\text{Gyr} - 0.2$ Gyr. Meanwhile, without stellar feedback, the mass loading factor is much smaller ($\eta \sim 0.01$), and no net outflow is observed. Hence, we conclude that stellar feedback drives strong gas outflow.

C. Decoupling of Instantaneous Outflow and Dark Matter Slope Variation

Past studies have shown that the outflowing gas can interact with dark matter by changing the gravitational potential and enabling dark matter particles to spread outwards, thus flattening the central cusp of the dark matter density profile. Our simulations adopt a much higher resolution that can directly resolve SN feedback without the sub-grid uncertainties, providing robust results and important confirmation that SN feedback is capable of changing the inner slope of dark matter halos.

We observe that the outflow is decoupled from the variation of the dark matter slope. Although the outflow of gas is episodic, the change in the density profile power law exponent γ is gradual. However, by comparing Simulation I with Simulation II, it is still clear that gas outflow is crucial to core formation.